Dynamic Modelling of Tetrazolium Based Microbial Toxicity Assay – A Parametric Proxy of Traditional Dose-Response Relationship

Chris Daniel Philus[1], Biswanath Mahanty[1,*]

[1] Department of Biotechnology, Karunya Institute of Technology and Sciences, Coimbatore, Tamil Nadu - 641114, India

* Corresponding author Email: bmahanty@karunya.edu

Abstract

Microbial toxicity of test substances in tetrazolium assay is often quantified while referring to IC_{50} values. However, the implication of such estimates is very limited and can differ across studies depending on prevailing test conditions. In this work, a factorial design-based end-point microbial assay was adopted, which suggests significant interaction (P= 0.041) between inoculum and tetrazolium dose on formazan production. A dynamic model framework was proposed to be incorporated in toxicity assay, that not only captures the nonlinear interdependency between biomass, substrate, formazan content but also measure the toxicity in terms of inhibition parameter. Microbial growth, glucose uptake, formazan production in presence and absence of heavy metal toxicant (Cu^{2+}) in designed batch studies were utilized for sequential estimation of model parameters and their bootstrap confidence intervals. A logistic growth model (R^2>0.96) with multiplicative inhibition terms fit the experimental data reasonably well. Dynamic relative sensitivity analysis revealed that both microbial growth and formazan production profiles were sensitive to toxicant inhibition parameter. The adoption of a dynamic model framework as a stable index for the toxic potential of test substances can be extended to design a versatile, robust in-vitro assay system.

Keywords: Dynamic Model; Heavy metals; Formazan; Sensitivity analysis; Tetrazolium; Microbial toxicity

1. Introduction

Evaluation of toxicity for new molecules, formulation, materials, toxicants or xenobiotics using appropriate organism is an integral part of risk characterization and assessment (Gabrielson et al. 2003; Wadhia et al. 2007). Biological assay systems with a microorganism, invertebrates, plants, or higher organisms have been used to measure the change in test organism or its response in presence of the toxicant in a quantitative manner (Iqbal 2016; Bartlett et al. 2017; Özgür et al. 2018; Luan et al. 2020). Toxicity assay using microbes as bioindicators remained simple, fast, versatile, reproducible, and can be extended to environmental, food, or biomedical applications (Polo et al. 2011; Hassan et al. 2016). Depending on the microorganism, environment and biological response, appropriate analytical techniques such as respirometric (Vasiliadou et al. 2018), fluorescent and luminescent bioassays (Roslev et al. 2015; Abbas et al. 2018), microbial fuel cell-based sensor (Dávila et al. 2011), methanogenic activity assay (Gonzalez-Estrella et al. 2013), microbial growth (Baek and An 2011) can be adopted.

Microbial reduction of tetrazolium has been widely used to measure microbial metabolic activity in toxicity assay (Wang et al. 2010; Lupu and Popescu 2013; van Tonder et al. 2015). The prototype 2,3,5-triphenyl-tetrazolium chloride (TTC) is one of widely studied redox indicator, which gets reduced into water-insoluble red formazan by microbial dehydrogenase in metabolically active cell (Junillon et al. 2014; Sabaeifard et al. 2014). The amount formazan extracted from the microbial cells grown in presence of toxicants would be lower than that of the control (Sydow et al. 2018). The inhibition of tetrazolium reduction with increasing dose of toxicant has also been used to assign a numerical indicator of the pollutant *e.g.* IC50 value- the effective concentration causing 50% reduction in measured response (Ma et al. 2018).

Despite being rapid and simple, selection of time for final reading in endpoint assay require optimization of the whole experiment (Stefanowicz-Hajduk and Ochocka 2020). In some cases, IC50 for a 24-hr incubation period can be different from 48-h incubation. A toxicant cannot be

tagged with a unique IC50 value as the outcome of tetrazolium assay depends on a multitude of interacting variables, such as the initial concentration of microorganism, substrate, TTC, and the incubation time (Ghaly and Mahmoud 2007; Sylvester 2011). The formazan yield has been known to increase with TTC concentration but beyond a critical point the yield declines (Ghaly and Mahmoud 2007). Assumption of a proportional relation between the amount of formazan deposit to the number or activity of living cells has already been questioned (Etxeberria et al. 2011). Intracellular accumulation of formazan can compromise the integrity of the plasma membrane (Bernas and Dobrucki 2004; Lü et al. 2012) and cell viability.

Accumulated formazan is a result of non-linear dynamics of substrate consumption, microbial growth, and toxicity of formazan as well as an external toxicant, integrated over the incubation period. Constant rate of formazan production can only be presumed when kinetics is known in a priori (Januszek et al. 2015; Małachowska-Jutsz and Matyja 2019). Substrate inhibition models based on modified Michaelis-Menten kinetics or empirical variants have also been adopted to explain TTC reduction data (Ghaly and Mahmoud 2007). The inhibition constant or parameters estimated for toxicants while modelling of temporal change in biomass, substrate, formazan concentration can be an invaluable static, toxicity indicator, resilience to variation incurred in endpoint toxicity assay.

In this study, a comprehensive dynamic model was developed to simulate the temporal change in biomass, substrate, formazan concentration during a toxicity assay. Model parameters were sequentially estimated using independent experimental data sets, designed to explore incremental subspace of complex model hierarchy. Appropriate kinetics (and parameters) for growth and substrate consumption were selected from a set of representative models that corroborate experimental data. The model fitness was ascertained using cross-validation, and the confidence intervals (CIs) of all estimated parameters, their sensitivities were also evaluated.

2. Materials and methods

2.1. Chemical, Microbial culture Media

Nutrient-broth for growth/maintenance of *E. coli* was purchased from HiMedia Co (Mumbai, India). Tetrazolium salt, 2,3,5-triphenyl-2H-tetrazolium chloride (TTC) for microbial toxicity assay was purchased from Sigma-Aldrich, India. Methanol and ethanol were purchased from SRL laboratories, Mumbai, India. Ultra-filtered Milli-Q® water (Millipore, Molsheim, France) was used for the preparation of the solutions. The components of Bushnell Haas (BH) mineral media in g l^{-1}: $MgSO_4$, 0.20; $CaCl_2$, 0.02; KH_2PO_4, 1.00; K_2HPO_4, 1.000, NH_4NO_3, 1.00; $FeCl_3$ 0.050; were purchased from Loba Chemie®, Mumbai, India.

2.2. Media preparation, culture growth and toxicity assay conditions

Overnight grown fresh *Escherichia coli* (ATCC 25922) in sterile nutrient broth medium centrifuged at 3500 × g for 15 min, re-dispersed in distilled water, was used as the test microorganism in all toxicity studies. Autoclaved BH media (pH 7) supplemented with filter-sterilized glucose stock (10 g l^{-1}) was used for further studies. TTC and $CuSO_4$, if required in experimental sets, were added from the aqueous stock solution (5 g l^{-1}, 50 mg l^{-1}, respectively).

2.2. Influence of initial biomass, glucose, TTC on tetrazolium reduction

Influence of biomass concentration (X_1), glucose (X_2), and TTC dosage (X_3) on tetrazolium reduction was evaluated by adopting a 2^3 full factorial experimental design as in **Table 1**. Different volume freshly grown (and resuspended) *E. Coli* culture, glucose and TTC solution was transferred into a set of 15 ml-sterile centrifuge tubes. The tubes were wrapped with aluminium foil, incubated in a shaker incubator for 2 h under dark condition. Following centrifugation at 3500 *g* for 10 min, the cell palette was processed for formazan extraction and analysis. Analysis of variance was carried out to determine the individual effects as well as the

interaction effects of the factors on the responses. Data processing and plotting were carried out using the software Minitab 18.

2.3. Experimental design for the discretization of dynamic model

The purpose of the design is to explore temporal change in microbial growth, glucose consumption, and TTC production (in presence or absence of toxic chemical), which can be used to model the dynamic behaviour of the process. The experiment was independently conducted in sets of 100-ml Erlenmeyer flasks with 50 ml of BH media (Table 2). Glucose was added at final concertation of 1 g l^{-1}, while 2 ml TTC (5 g l^{-1} stock) and 250 µl $CuSO_4$ (50 mg l^{-1}) were added if included in the design. All flasks were incubated at 37ºC in a shaker incubator for 16 h. On every 2 h interval, 2 ml sample was collected, optical density was measured at 600 nm, and kept in the refrigerator for further analysis. After completion of the experiment, samples were centrifuged at 3500 *g* for 15 min, the supernatant was collected for residual glucose analysis and cell palette was processed for formazan extraction.

2.4. Analytical Methods

The optical densities of the samples were measured at 600 nm (path length 1 cm) using a UV–visible spectrophotometer. The measurements were converted to dry-weight based biomass concentration (in g l^{-1}) using a standard prepared in the identical range of concentrations.

calibration Residual glucose concentration in the culture supernatant was measured using dinitro-salicylic acid (DNSA) method (Kona et al. 2001) using a standard curve prepared with known glucose concentration (0.2-1 g l^{-1}).

Concentrated HCl (20 µl) was added to cell palette to release intracellular formazan, which was dissolved in 2 ml methanol (Lopez Del Egido et al. 2017). The sample extract was centrifuged at 3500 *g* for 10 min and absorbance of supernatants were recorded 480 nm against reagent blank.

138 *2.5. Biomass growth, substrate consumption and Toxicity modelling*

139 2.5.1. Formulation of model structure

140 Microbial growth on glucose is assumed to be substrate limited process, and a flexible and
141 generalized rate expression is preferred. High formazan concentration (F) and/or presence of
142 toxicant (M) is assumed to inhibit microbial growth, where the increasing concentration of
143 formazan crystal inside a cell can reduce viability. That phenomenon can be modelled as
144 product inhibition perspective (Lin et al. 2008) as shown in generalized specific growth rate
145 expression as in Eq. 1.

146 $$\mu = \mu_G \left(\frac{K_F}{K_f + r_{F/X}} \right) \left(\frac{K_m}{K_m + M} \right) \quad (1)$$

147 Where μ_g is a mathematical expression for glucose-limited microbial growth (explained later).
148 The second and third terms on the right-hand side represent growth inhibition due to formazan,
149 and toxicant (e.g., heavy metal), respectively. The $r_{F/X}$ is the relative concentration of formazan
150 (F) to biomass (X) and K_f is the inhibition constant. The inhibition effect would be negligible
151 at an early phase of incubation when biomass accumulated formazan concentration is very low
152 (i.e., $r_{F/X} \approx 0$). However, at a very high level of intracellular formazan (i.e., $r_{F/X} >> K_f$), the
153 growth rate becomes inversely proportional to formazan content. The K_m is inhibition constant
154 for the toxicant – a dose that would cause a 50% reduction in microbial growth rate than in the
155 toxicant free environment. The spiked toxicant in the present study is heavy-metal, that is not
156 degraded metabolized, and hence its concentration (M) is assumed to remain constant, time-
157 invariant.

158 The dynamic change in biomass, glucose, and formazan concentration is given by Eq. 2-4.

159 $$\frac{dX}{dt} = \mu X \quad (2)$$

160 $$\frac{dG}{dt} = -\frac{1}{Y_{X/G}}\frac{dX}{dt} - \beta X \quad (3)$$

161 $$\frac{dF}{dt} = \begin{cases} \gamma \frac{dX}{dt} + \delta X & F < F_{\max} \\ 0 & F = F_{\max} \end{cases} \quad (4)$$

162 Glucose consumption and formazan production are (from tetrazolium reduction) modelled as
163 growth associated or non-associated process as in Eq. 3 and 4, respectively. The term $Y_{X/G}$ on
164 the right-hand side in Eq. 3 represent true biomass yield coefficient, while the second term (β)
165 represents maintenance requirement. The rate of formazan production ceases once formazan
166 concentration attains its theoretical asymptotic maximum (F_{max}) assuming 1:1 molar reduction
167 of added tetrazolium in the culture broth.

168 2.5.2. Selection of Growth model

169 In absence of tetrazolium/formazan or heavy metals, the glucose-limited growth of
170 microorganism μ_G was modelled using Logistic, Monod, Contois, and Tessier kinetics as
171 represented in Equations 5a-5d, respectively

172 $$\mu_G = \mu_m \left(1 - \frac{X}{X_{\max}}\right) \quad (5a)$$

173 $$\mu_G = \frac{\mu_m G}{K_d + G} \quad (5b)$$

174 $$\mu_G = \frac{\mu_m G}{K_c X + G} \quad (5c)$$

175 $$\mu_G = \mu_m \left(1 - \exp\left(-G/K_t\right)\right) \quad (5d)$$

176 Where $X_{\max}$ is the asymptotic biomass concentration in logistic growth. The K_d, K_c, K_t are
177 kinetic constant relevant to Monod, Contois and Tessier models.

178 2.5.3. Formulation of the dynamic model and parameter estimation strategy

179 A complete set of coupled ordinary differential equations (ODEs) reflecting the rate of change
180 for all state variables is shown in Eqs. (1)–(5). Simultaneous estimation of all eight parameters
181 from a single experimental data set using biomass, glucose and formazan concentration profiles
182 could be inherently inaccurate. A discretized approach, where only a subset of parameters is
183 required to be estimated from the hierarchical model subspace, utilizing the data from a
184 designed experiment (Table 2), was adopted as outlined in following steps.

185 **Step 1.** Experimental set containing only biomass, glucose data were used to select the ideal
186 growth model (i.e., Logistic, Monod, Contois, or Tessier) as well as their relevant parameters.
187 The inhibition terms for formazan and toxicant as in Eq. 1 can be dropped.

188 **Step 2.** Experimental set containing biomass, glucose, formazan data was used to estimate
189 growth inhibition term (K_F) in Eq. 1, and formazan production parameters (γ, δ). Growth related
190 parameters were adopted from an earlier step, the biomass yield coefficient or maintenance
191 requirement of glucose ($Y_{X/G}$, β) was re-calibrated.

192 **Step 3.** Experimental set containing biomass, glucose, formazan, and toxicant was used to
193 estimate growth inhibition term (K_m) in Eq. 1 while adopting all other parameters from step 2.
194 The numerical solution of the dynamic model was approached from an initial value state
195 variable and reasonable guess of parameters (within suitable space boundaries) in Matlab®
196 ode45 solver. Subsequently, a normalized residual sum of squares (NSSE) between
197 experimental and modelled profiles was minimized (Eq. 6) while changing relevant
198 parameter(s) in a constrained minimization algorithm using *fmincon* function in Matlab®.
199

200 $$NSSE = \sum_{i=1}^{u} \left(\frac{\sum_{j=1}^{n} \left(x_{i,j} - \hat{x}_{i,j} \right)^2}{\sum_{j=1}^{n} \left(x_{i,j} - \overline{x}_i \right)^2} \right) \quad (6)$$

201 where u is the number of measured state variables (i.e., two or three in this study), n is the
202 number of data points in each measured ($x_{i,j}$) or modelled ($\hat{x}_{i,j}$) profiles. The $\overline{x}$ is the
203 average measured value of the i_{th} profile.

204 2.5.4. Cross-validation, confidence interval estimation and sensitivity

205 As a check against overfitting, and to assess the model's ability to predict data not used in
206 model fitting (i.e., its capacity for out-of-sample prediction), a five-fold cross-validation
207 analysis was carried out and coefficient of determination (R^2_{cv}) was estimated. The confidence
208 interval (CI) for parameter estimates in the dynamic model data was processed using a residual-
209 based, non-parametric bootstrap resampling approach (Dogan 2007). The dynamic relative
210 sensitivity, i.e. relative sensitivity at different time intervals, for the model parameters was
211 calculated using the finite difference approximation (Yue et al. 2006) with a repeated solution
212 (twice) of the model for each parameter. The sensitivity analysis represented here is essentially
213 a univariate, where a change in modelled responses (e.g., biomass, substrate, product) is
214 mapped from the perturbation of single parameter value while keeping other parameters on
215 hold at their original estimate. Local relative sensitivity as a function of time allows a direct
216 comparison of responses at different states or across different parameters (Eq. 7).

217 $$\overline{s}_{i,j,t} = \frac{\partial y_{i,t} / y_{i,t}}{\partial \theta_j / \theta_j} \quad (7)$$

218 where $y_{i,t}$ is the i^{th} response at time t and θ_j is the j^{th} parameter of which sensitivity is being
219 measured.

220

3. Results and Discussions

3.1. Impact of initial biomass, substrate, and tetrazolium on formazan concentration

A factorial analysis was performed on the data to study the influence of inoculum size, glucose concentration, TTC dose and their interactions on formazan production and the results are presented in Table 3. Analysis of variance performed on the data set (Table 4) revealed that inoculum size and TTC dose and their 2-way interactions did significantly affect formazan production ($P<0.05$). This is also supported by the Pareto chart (Fig.1) showing order of influencing parameters. The plots for individual factor effects on formazan productivity showed that increasing amounts of inoculum was favourable while increasing amount of glucose or TTC can inhibit actively growing microbial culture, resulting in lower TTC reduction into formazan. Similar toxic effect of tetrazolium salts has been made in previous studies (Junillon and Flandrois 2014). A reversible increase in the duration of lag phase has also been observed for gram-positive *Listeria monocytogenes* culture growing in presence of different tetrazolium salts (Junillon and Flandrois 2014).

3.2. Dynamic model parameters in toxicity assay

The microbial biomass and glucose concentration profile from experimental sets without TTC or toxicant (i.e., cupper salt) were modelled using Logistic growth, Monod, Contois, and Tessier models. The fitness of the chosen models against experimental data has been shown in Table 5. The overall fitness of the logistic model to biomass or substrate profiles (respective R^2 of 0.9663, 0.9633) is better than the other three models. It should be noted that the biomass growth is not coupled with substrate concertation in the Logistic model structure, but the substrate depletion is proportion to biomass growth. The logistic model has successfully been used to explain growth and substrate consumption by *E. coli* in batch studies under substrate

limited conditions (Li et al. 2010; Wittgens et al. 2011) or population growth model in microbial culture in toxicity assay (E. Lindstrom et al. 1998).

The experimental and modelled profiles (for biomass, substrates and formazan) are also shown in **Fig. 2**, depicting the suitability of the selected kinetics for modelling observations in toxicity assay. The modelled profiles are in good agreement with experimental data, except for substrate concentration which is somehow over-predicted at the late phase in a batch experiment involving both TTC and toxicants.

The least-square estimates of substrate consumption, formazan production and microbial growth inhibition (due to formazan and toxicant) parameters along with their boot-strap CIs are presented in **Table 6**. The high cross-validation R^2 for both biomass and substrate concentration profiles suggests no over-prediction in the proposed logistic growth model. Certainly, the estimates for μ_{max} (0.3674 h^{-1}) and X_{max} (1.2658 g l^{-1}) can be extended to other experimental sets containing TTC and/or cupper, as long as the growth-limiting substrate remains identical. However, estimates biomass yield and maintenance coefficient can change in presence of formazan and/or toxicant (Şengör et al. 2009). Those parameters were recalibrated from additional experimental sets containing inhibitor /toxicants. It should be noted that all parameters were not estimated from a single batch experiment, rather sequentially estimated that improves the accuracy (Wang et al. 2018).

The biomass growth yield coefficient (0.747 g g^{-1}) and formazan inhibition constant K_F, (30.963 mg g^{-1}) were estimated from experimental sets containing glucose, and TTC. The yield coefficient estimates seem to be in the same order of growth-associated stoichiometric true yield coefficient (0.57 g g^{-1}) as reported for *E. coli* in glucose-limited continuous culture (Kayser et al. 2005). It should be noted that the biomass yield coefficient reported in the present study does not consider the corrections for the maintenance requirement. Though literature advocates bacterial growth inhibition in presence of tetrazolium salts (Villegas-Mendoza et al.

2015), no attempts (either mechanistic or empirical) has been made to model the kinetics of formazan toxicity. No comparison or discussions on the estimate of K_F (30.963 mg g^{-1}) can be made in the light of existing literature.

The estimates formazan production parameters (γ and δ respectively) suggests the process be primarily growth associated one. The non-growth associated formazan production rate ($1.257e^{-05}$ mg g^{-1} h^{-1}) is very trivial and accumulated intracellular formazan within the incubation period for in-vitro toxicity assay is likely to be far below than the K_F. In other words, non-growth associated formazan production alone cannot exert any toxicity. A significant positive relationship between specific growth rate and formazan production rate has also been reported in other studies (Villegas-Mendoza et al. 2019). Though formazan production in batch cultures increases with time, the formazan production rate decreases more rapidly.

The inhibition parameter pertinent to metal toxicity has been estimated to be 152.39 mg l^{-1} from the third batch study containing TTC as well as Cu^{+2}. The regression coefficients for biomass, substrate and formazan concentration profiles (0.856, 0.782, 0.964) in this least square estimation exercise were inferior in comparison to the other two batches. This could be attributed to constrained parameter subspace for K_m, as all other parameters were already pre-fixed, leaving a lower degree of freedom. Utgikar et al modelled toxicity of copper on sulfate-reducing mixed microbial cultures at two perspectives, i.e., a toxic effect causing the death of cells or inhibitory effect using an inverse exponential function (Utgikar et al. 2003). The author reported inhibition constant 1140 mg l^{-1} for copper, which is about 10-fold higher than the current estimate. The reported half inhibitory concentrations (IC_{50}) for Cu(II) in enzymatic or respirometric assays vary widely (<0.2 to 200 mg l^{-1}) in the literature (Esquivel-Rios et al. 2014). This difference or discrepancy is very logical considering the variance in microbial culture, test conditions and the mathematical model adopted.

293 *3.3. Bootstrap parameter distribution and sensitivity*

294 The distribution of bootstrap parameters in the proposed toxicity model is shown in **Fig. 3**,
295 where a near symmetric normal/gaussian distribution for μ_{max}, X_{max} (from glucose consumption
296 and biomass growth data) assures better credibility. The distribution of parameters such as K_F
297 and $Y_{X/G}$ are somewhat right-skewed, which can be related to the inaccuracy of the estimate,
298 or poor parameter sensitivity. The distribution of γ and K_m exhibits a marginal left-skewness,
299 implying the presence of outlier in experimental data(Joshi et al. 2006). Such deviation can be
300 linked to the hierarchical parameter estimation approach and nonlinearity of the dynamic
301 model.

302 Sensitivity analysis of the toxicity model parameters on biomass, substrate, and formazan
303 content is shown in Fig. 4. The relative sensitivities of the different parameters not only vary
304 between profiles but also with time for a given response. The growth profile appears to be most
305 sensitive toward μ_{max}, K_f, K_m. This is very logical as the specific growth rate is directly
306 dependent on those parameters. Moreover, the relative sensitivities have been shown to
307 increase with time. This can be attributed to a higher amount of accumulated biomass and
308 formazan at later phase of microbial growth. As the growth model is not directly coupled with
309 substrate consumption, growth data remains insensitive to β, δ, or $Y_{X/G}$. The negative relative
310 sensitivity of substrate profiles with X_{max} reflects faster depletion of the substrate. The substrate
311 consumption profile remains insensitive to β, δ, which are non-growth associated parameters
312 for glucose consumption or formazan production, respectively. Entire sets of parameters that
313 had a significant influence on growth (i.e., μ_{max}, K_f, K_m, γ) appears to impact formazan
314 production as well. However, the sensitivity of γ on the formazan profile is positive which is
315 very reasonable from their kinetic relationship. As formazan content increases, the absolute
316 sensitivity of γ declines over time. Conceivably, parameters in the dynamic model are

317 temporarily separated where any parameter(s) relevant to a later stage does not influence the
318 preceding process responses.

319 *3.4. External Validation of the Proposed Model*

320 A dynamic model for toxicity assay was validated using an independent TTC free experimental
321 set spiked with 50 mg l^{-1} Cu^{2+} while keeping the other process conditions unchanged. The
322 experimental and modelled data for biomass and residual glucose concentrations are presented
323 in Fig. 5. The experimental and modelled data were in close agreement, particularly at the
324 initial growth phases. However, at the later stage, experimental biomass and glucose profiles
325 drifted toward the lower and higher side respectively as compared to the model. Although an
326 explanation for such discrepancies is not available, such deviations were within reasonable
327 limits of uncertainty due to measurement error.

328 **4. Conclusions**

329 Mathematical formalization of tetrazolium based microbial toxicity assay and projection of
330 estimated kinetic model parameter as an invariable and reproducible alternative to traditional
331 toxicity assay reporting has been proposed. Growth inhibition was modelled as a function of
332 intracellular formazan content and toxicant concentration. Parameters, sequentially estimated
333 from batch experimental data, were credible with narrow confidence intervals. Though a
334 limited combination of growth, substrate consumption and inhibition models were only
335 adopted in this study, the approach can easily be extrapolated to much larger and multivariate
336 data set incorporating mechanistic insight of the toxicity assay. Parametric representation of
337 result can offer a unified format of reconciliation, reporting and validation for in-vitro toxicity
338 assay.

339 **Acknowledgements**

Standard ethical and professional conduct have been followed. There are no conflicts of interests (financial or otherwise) associated with this publication.

Declarations

Ethics approval and consent to participate

The study does not involve any human participants, human data or human tissue. Ethics approval is not applicable.

Consent for publication

N/A

Availability of data and materials

Experimental the data in this study are available on request to corresponding author.

Competing interests

None

Funding

This work is financially supported by Karunya Institute of Technology and Sciences.

Authors' contributions

BM conceived and designed the experiments. CDF performed the experiments and sample analysis. BM and CDF analyzed the data for modelling. CDF and BM drafted the manuscript. All authors revise and approve and manuscript.

359 **References**

360 Abbas M, Adil M, Ehtisham-ul-Haque S, et al (2018) Vibrio fischeri bioluminescence
361 inhibition assay for ecotoxicity assessment: A review. Sci Total Environ 626:1295–1309.
362 https://doi.org/10.1016/j.scitotenv.2018.01.066
363 Baek Y-W, An Y-J (2011) Microbial toxicity of metal oxide nanoparticles (CuO, NiO, ZnO,
364 and Sb2O3) to Escherichia coli, Bacillus subtilis, and Streptococcus aureus. Sci Total
365 Environ 409:1603–1608. https://doi.org/10.1016/j.scitotenv.2011.01.014
366 Bartlett AJ, Frank RA, Gillis PL, et al (2017) Toxicity of naphthenic acids to invertebrates:
367 Extracts from oil sands process-affected water versus commercial mixtures. Environ
368 Pollut 227:271–279. https://doi.org/10.1016/j.envpol.2017.04.056
369 Bernas T, Dobrucki JW (2004) Backscattered light confocal imaging of intracellular MTT-
370 formazan crystals. Microsc Res Tech 64:126–134. https://doi.org/10.1002/jemt.20070
371 Dávila D, Esquivel JP, Sabaté N, Mas J (2011) Silicon-based microfabricated microbial fuel
372 cell toxicity sensor. Biosens Bioelectron 26:2426–2430.
373 https://doi.org/10.1016/j.bios.2010.10.025
374 Dogan G (2007) Bootstrapping for confidence interval estimation and hypothesis testing for
375 parameters of system dynamics models. Syst Dyn Rev 23:415–436.
376 https://doi.org/10.1002/sdr.362
377 E. Lindstrom J, P. Barry R, Braddock JF (1998) Microbial community analysis: a kinetic
378 approach to constructing potential C source utilization patterns. Soil Biol Biochem
379 30:231–239. https://doi.org/10.1016/S0038-0717(97)00113-2
380 Esquivel-Rios I, González I, Thalasso F (2014) Microrespirometric characterization of
381 activated sludge inhibition by copper and zinc. Biodegradation 25:867–879.
382 https://doi.org/10.1007/s10532-014-9706-1
383 Etxeberria A, Mendarte S, Larregla S (2011) Determination of viability of Phytophthora capsici

384 oospores with the tetrazolium bromide staining test versus a plasmolysis method. Rev
385 Iberoam Micol 28:43–49. https://doi.org/10.1016/j.riam.2010.11.005
386 Gabrielson J, Kühn I, Colque-Navarro P, et al (2003) Microplate-based microbial assay for risk
387 assessment and (eco)toxic fingerprinting of chemicals. Anal Chim Acta 485:121–130.
388 https://doi.org/10.1016/S0003-2670(03)00404-5
389 Ghaly AE, Mahmoud NS (2007) Effects of tetrazolium chloride concentration, O2, and cell
390 age on dehydrogenase activity of Aspergillus niger. Appl Biochem Biotechnol 136:207–
391 222. https://doi.org/10.1007/BF02686018
392 Gonzalez-Estrella J, Sierra-Alvarez R, Field JA (2013) Toxicity assessment of inorganic
393 nanoparticles to acetoclastic and hydrogenotrophic methanogenic activity in anaerobic
394 granular sludge. J Hazard Mater 260:278–285.
395 https://doi.org/10.1016/j.jhazmat.2013.05.029
396 Hassan SHA, Van Ginkel SW, Hussein MAM, et al (2016) Toxicity assessment using different
397 bioassays and microbial biosensors. Environ Int 92–93:106–118.
398 https://doi.org/10.1016/j.envint.2016.03.003
399 Iqbal M (2016) Vicia faba bioassay for environmental toxicity monitoring: A review.
400 Chemosphere 144:785–802. https://doi.org/10.1016/j.chemosphere.2015.09.048
401 Januszek K, Długa J, Socha J (2015) Dehydrogenase activity of forest soils depends on the
402 assay used. Int Agrophysics 29:47–59. https://doi.org/10.1515/intag-2015-0009
403 Joshi M, Seidel-Morgenstern A, Kremling A (2006) Exploiting the bootstrap method for
404 quantifying parameter confidence intervals in dynamical systems. Metab Eng 8:447–455.
405 https://doi.org/10.1016/j.ymben.2006.04.003
406 Junillon T, Flandrois J-P (2014) Diminution of 2,3,5-triphenyltetrazolium chloride toxicity on
407 Listeria monocytogenes growth by iron source addition to the culture medium. Food
408 Microbiol 38:1–5. https://doi.org/10.1016/j.fm.2013.07.005

409 Junillon T, Morand L, Flandrois JP (2014) Enhanced tetrazolium violet reduction of
410 Salmonella spp. by magnesium addition to the culture media. Food Microbiol 42:132–
411 135. https://doi.org/10.1016/j.fm.2014.03.008
412 Kayser A, Weber J, Hecht V, Rinas U (2005) Metabolic flux analysis of Escherichia coli in
413 glucose-limited continuous culture. I. Growth-rate-dependent metabolic efficiency at
414 steady state. Microbiology 151:693–706. https://doi.org/10.1099/mic.0.27481-0
415 Kona RP, Qureshi N, Pai JS (2001) Production of glucose oxidase using Aspergillus niger and
416 corn steep liquor. Bioresour Technol 78:123–126. https://doi.org/10.1016/S0960-
417 8524(01)00014-1
418 Li Q, Wang D, Wu Y, et al (2010) Kinetic evaluation of products inhibition to succinic acid
419 producers Escherichia coli NZN111, AFP111, BL21, and Actinobacillus succinogenes
420 130ZT. J Microbiol 48:290–296. https://doi.org/10.1007/s12275-010-9262-2
421 Lin SKC, Du C, Koutinas A, et al (2008) Substrate and product inhibition kinetics in succinic
422 acid production by Actinobacillus succinogenes. Biochem Eng J 41:128–135.
423 https://doi.org/10.1016/j.bej.2008.03.013
424 Lopez Del Egido L, Navarro-Miró D, Martinez-Heredia V, et al (2017) A Spectrophotometric
425 Assay for Robust Viability Testing of Seed Batches Using 2,3,5-Triphenyl Tetrazolium
426 Chloride: Using Hordeum vulgare L. as a Model. Front Plant Sci 8:.
427 https://doi.org/10.3389/fpls.2017.00747
428 Lü L, Zhang L, Wai MSM, et al (2012) Exocytosis of MTT formazan could exacerbate cell
429 injury. Toxicol Vitr 26:636–644. https://doi.org/10.1016/j.tiv.2012.02.006
430 Luan X, Liu X, Fang C, et al (2020) Ecotoxicological effects of disinfected wastewater
431 effluents: a short review of in vivo toxicity bioassays on aquatic organisms. Environ Sci
432 Water Res Technol. https://doi.org/10.1039/D0EW00290A
433 Lupu ARR, Popescu T (2013) The noncellular reduction of MTT tetrazolium salt by TiO2

nanoparticles and its implications for cytotoxicity assays. Toxicol Vitr 27:1445–1450. https://doi.org/10.1016/j.tiv.2013.03.006

Ma Y, Li X, Mao H, et al (2018) Remediation of hydrocarbon–heavy metal co-contaminated soil by electrokinetics combined with biostimulation. Chem Eng J 353:410–418. https://doi.org/10.1016/j.cej.2018.07.131

Małachowska-Jutsz A, Matyja K (2019) Discussion on methods of soil dehydrogenase determination. Int J Environ Sci Technol 16:7777–7790. https://doi.org/10.1007/s13762-019-02375-7

Özgür ME, Balcıoğlu S, Ulu A, et al (2018) The in vitro toxicity analysis of titanium dioxide (TiO 2) nanoparticles on kinematics and biochemical quality of rainbow trout sperm cells. Environ Toxicol Pharmacol 62:11–19. https://doi.org/10.1016/j.etap.2018.06.002

Polo AM, Tobajas M, Sanchis S, et al (2011) Comparison of experimental methods for determination of toxicity and biodegradability of xenobiotic compounds. Biodegradation 22:751–761. https://doi.org/10.1007/s10532-010-9448-7

Roslev P, Lentz T, Hesselsoe M (2015) Microbial toxicity of methyl tert-butyl ether (MTBE) determined with fluorescent and luminescent bioassays. Chemosphere 120:284–291. https://doi.org/10.1016/j.chemosphere.2014.07.003

Sabaeifard P, Abdi-Ali A, Soudi MR, Dinarvand R (2014) Optimization of tetrazolium salt assay for Pseudomonas aeruginosa biofilm using microtiter plate method. J Microbiol Methods 105:134–140. https://doi.org/10.1016/j.mimet.2014.07.024

Şengör SS, Barua S, Gikas P, et al (2009) Influence of Heavy Metals on Microbial Growth Kinetics Including Lag Time: Mathematical Modeling and Experimental Verification. Environ Toxicol Chem 28:2020. https://doi.org/10.1897/08-273.1

Stefanowicz-Hajduk J, Ochocka JR (2020) Real-time cell analysis system in cytotoxicity applications: Usefulness and comparison with tetrazolium salt assays. Toxicol Reports

7:335–344. https://doi.org/10.1016/j.toxrep.2020.02.002

Sydow Z, Lisiecki P, Staninska-Pięta J, et al (2018) Multidimensional Toxicity of Rhamnolipid Extracts Obtained From Creosote-Contaminated Soil. CLEAN - Soil, Air, Water 46:1800053. https://doi.org/10.1002/clen.201800053

Sylvester PW (2011) Optimization of the Tetrazolium Dye (MTT) Colorimetric Assay for Cellular Growth and Viability. In: Methods in molecular biology (Clifton, N.J.). pp 157–168

Utgikar VP, Tabak HH, Haines JR, Govind R (2003) Quantification of toxic and inhibitory impact of copper and zinc on mixed cultures of sulfate-reducing bacteria. Biotechnol Bioeng 82:306–312. https://doi.org/10.1002/bit.10575

van Tonder A, Joubert AM, Cromarty AD (2015) Limitations of the 3-(4,5-dimethylthiazol-2-yl)-2,5-diphenyl-2H-tetrazolium bromide (MTT) assay when compared to three commonly used cell enumeration assays. BMC Res Notes 8:47. https://doi.org/10.1186/s13104-015-1000-8

Vasiliadou IA, Molina R, Martinez F, et al (2018) Toxicity assessment of pharmaceutical compounds on mixed culture from activated sludge using respirometric technique: The role of microbial community structure. Sci Total Environ 630:809–819. https://doi.org/10.1016/j.scitotenv.2018.02.095

Villegas-Mendoza J, Cajal-Medrano R, Maske H (2015) INT (2-(4-Iodophenyl)-3-(4-Nitrophenyl)-5-(Phenyl) Tetrazolium Chloride) Is Toxic to Prokaryote Cells Precluding Its Use with Whole Cells as a Proxy for In Vivo Respiration. Microb Ecol 70:1004–1011. https://doi.org/10.1007/s00248-015-0626-3

Villegas-Mendoza J, Cajal-Medrano R, Maske H (2019) The Chemical Transformation of the Cellular Toxin INT (2-(4-Iodophenyl)-3-(4-Nitrophenyl)-5-(Phenyl) Tetrazolium Chloride) as an Indicator of Prior Respiratory Activity in Aquatic Bacteria. Int J Mol Sci

20:782. https://doi.org/10.3390/ijms20030782

Wadhia K, Dando T, Clive Thompson K (2007) Intra-laboratory evaluation of Microbial Assay for Risk Assessment (MARA) for potential application in the implementation of the Water Framework Directive (WFD). J Environ Monit 9:953. https://doi.org/10.1039/b704059h

Wang H, Cheng H, Wang F, et al (2010) An improved 3-(4,5-dimethylthiazol-2-yl)-2,5-diphenyl tetrazolium bromide (MTT) reduction assay for evaluating the viability of Escherichia coli cells. J Microbiol Methods 82:330–333. https://doi.org/10.1016/j.mimet.2010.06.014

Wang Z, Sheikh H, Lee K, Georgakis C (2018) Sequential Parameter Estimation for Mammalian Cell Model Based on In Silico Design of Experiments. Processes 6:100. https://doi.org/10.3390/pr6080100

Wittgens A, Tiso T, Arndt TT, et al (2011) Growth independent rhamnolipid production from glucose using the non-pathogenic Pseudomonas putida KT2440. Microb Cell Fact 10:80. https://doi.org/10.1186/1475-2859-10-80

Yue H, Brown M, Knowles J, et al (2006) Insights into the behaviour of systems biology models from dynamic sensitivity and identifiability analysis: a case study of an NF-kappaB signalling pathway. Mol Biosyst 2:640–649. https://doi.org/10.1039/b609442b

Table 1. Factorial design to examine the dependence of TTC reduction on biomass, substrate and TTC concentration.

Factor	Units	Actual values at coded levels	
		-1	+1
Inoculum (X_1) OD@600 nm 0.196	ml	0.5	1.5
Glucose solution (10 g l^{-1}) added (X_2)	ml	0.1	0.3
TTC solution (5 g l^{-1}) added (X_3)	ml	0.05	0.10

Table 2. Hierarchical experimental design to decipher tetrazolium-based toxicity model

Exp. Set	Biomass	Glucose	TTC	$CuSO_4$	Parameters to be estimated for
1	+	+	-	-	Growth, substrate consumption
2	+	+	+	-	TTC reduction, and TTC toxicity
3	+	+	+	+	Test toxicant related parameters

511 **Table 3.** Factorial design matrix and formazan concentration

Sl. No:	Factors			Response
	E. coli culture (ml)	Glucose solution (ml)	TTC solution (ml)	Formazan content absorbance @480 nm
1	1.50	0.30	0.05	0.845
2	1.50	0.10	0.10	0.62
3	1.50	0.30	0.10	0.931
4	1.50	0.10	0.05	0.882
5	0.50	0.10	0.10	0.096
6	0.50	0.30	0.10	0.143
7	0.50	0.10	0.50	0.16
8	0.50	0.30	0.50	0.158

512

513

Table 4. Analysis of variance performed on the formazan production data.

Source	DF	Adj. SS	Adj. MS	F-Value	*P*-Value
Model	6	0.042879	0.007147	176.46	0.058
Linear	3	0.029382	0.009794	241.82	0.047
Inoculum	1	0.017861	0.017861	441.00	0.030*
Glucose	1	0.000421	0.000421	10.38	0.192
TTC	1	0.011101	0.011101	274.09	0.038*
2-Way Interactions	3	0.013498	0.004499	111.09	0.070
Inoculum * Glucose	1	0.003698	0.003698	91.31	0.066
Inoculum *TTC	1	0.009800	0.009800	241.98	0.041*
Glucose *TTC	1	0.000000	0.000000	0.00	1.000
Error	1	0.000040	0.000040		
Total	7	0.042920			

519 Table 5. Performance of different kinetic models fitting microbial growth and glucose
520 utilization data in absence of tetrazolium or toxicant.

Model	Associated Parameters *	Regression coefficients on profile for		
		Biomass	Substrate	Average
Logistic growth	μ_{max} = 0.3604; X_m = 1.2658 $Y_{X/S}$ = 4.2122; β = 0.0437	0.9602	0.9663	0.9633
Contois model	μ_{max} = 0.7819; K_c = 6.0312 $Y_{X/S}$ = 3.7230; β = 0.0409	0.9462	0.9713	0.9587
Tessier model	μ_{max} = 2.4161; K_t = 11.533 $Y_{X/S}$ = 1.5701; β = 0.0038	0.8560	0.9551	0.9055
Monod model	μ_{max} = 2.6378; K_d = 12.205 $Y_{X/S}$ = 1.5234; β = 0.0013	0.8602	0.9321	0.8962

521 * The units associated with parameters are h^{-1} (μ_{max}), $g.l^{-1}$ (X_m, K_d, K_t), and $g.g^{-1}$ ($Y_{X/S}$, K_c)
522

523 **Table 6.** The bootstrap confidence interval of parameter estimates for the dynamic model
524 structure at different modelling stages and the regression coefficients [$]

Exp. Sets	Parameters	R^2_{cal} (R^2_{cv})	Parameter Estimates	95% CI	
				Lower	Upper
Set-1	μ_{max} (h^{-1})	R^2_X = 0.960 (0.907)	0.360	0.296	0.429
	X_{max} (g l^{-1})	R^2_G = 0.966(0.915)	1.266	1.131	1.428
Set-2	K_F (mg g^{-1})	R^2_X = 0.958 (0.909)	30.963	26.738	37.126
	$Y_{X/G}$ (g g^{-1})	R^2_G = 0.975 (0.955)	0.747	0.659	0.793
	β (h^{-1})	R^2_F = 0.967 (0.933)	$8.778e^{-07}$	$8.192e^{-07}$	$9.015e^{-07}$
	γ (mg g^{-1})		20.641	19.02	23.81
	δ (mg h^{-1} g^{-1})		$1.257e^{-05}$	$1.173e^{-05}$	$1.295e^{-05}$
Set-3	K_m (mg l^{-1})	R^2_X = 0.856 (0.828)	152.39	141.68	186.49
		R^2_G = 0.782 (0.667)			
		R^2_F = 0.964 (0.913)			

525 [$] four-fold cross-validation R^2 (R^2_{CV}) with 10 Monte-Carlo repetitions for validation.

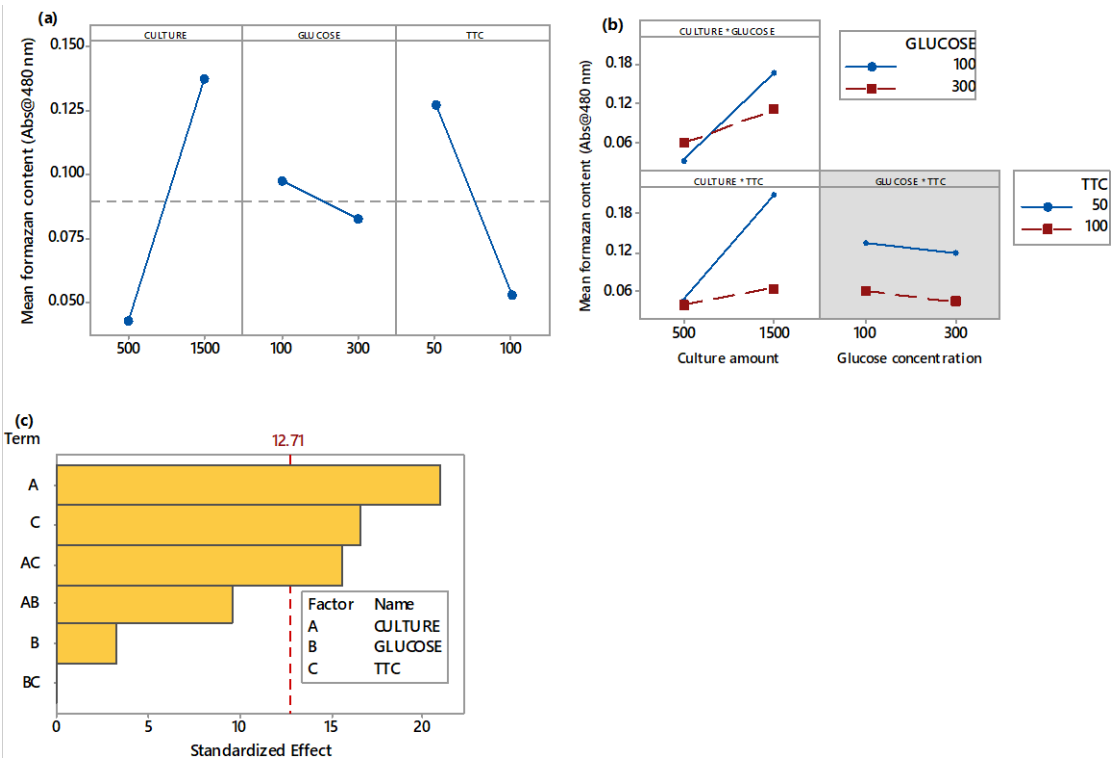

Figure 1. Influence of inoculum, glucose and TTC dose on formazan concentration as depicted in (a) main effect plot as a mean response, (b) interaction plot for each combination of two factors, and (c) Pareto chart where bars represent the absolute value of the effect of each factor and the dotted line indicates the limit of significance ($\alpha = 0.05$).

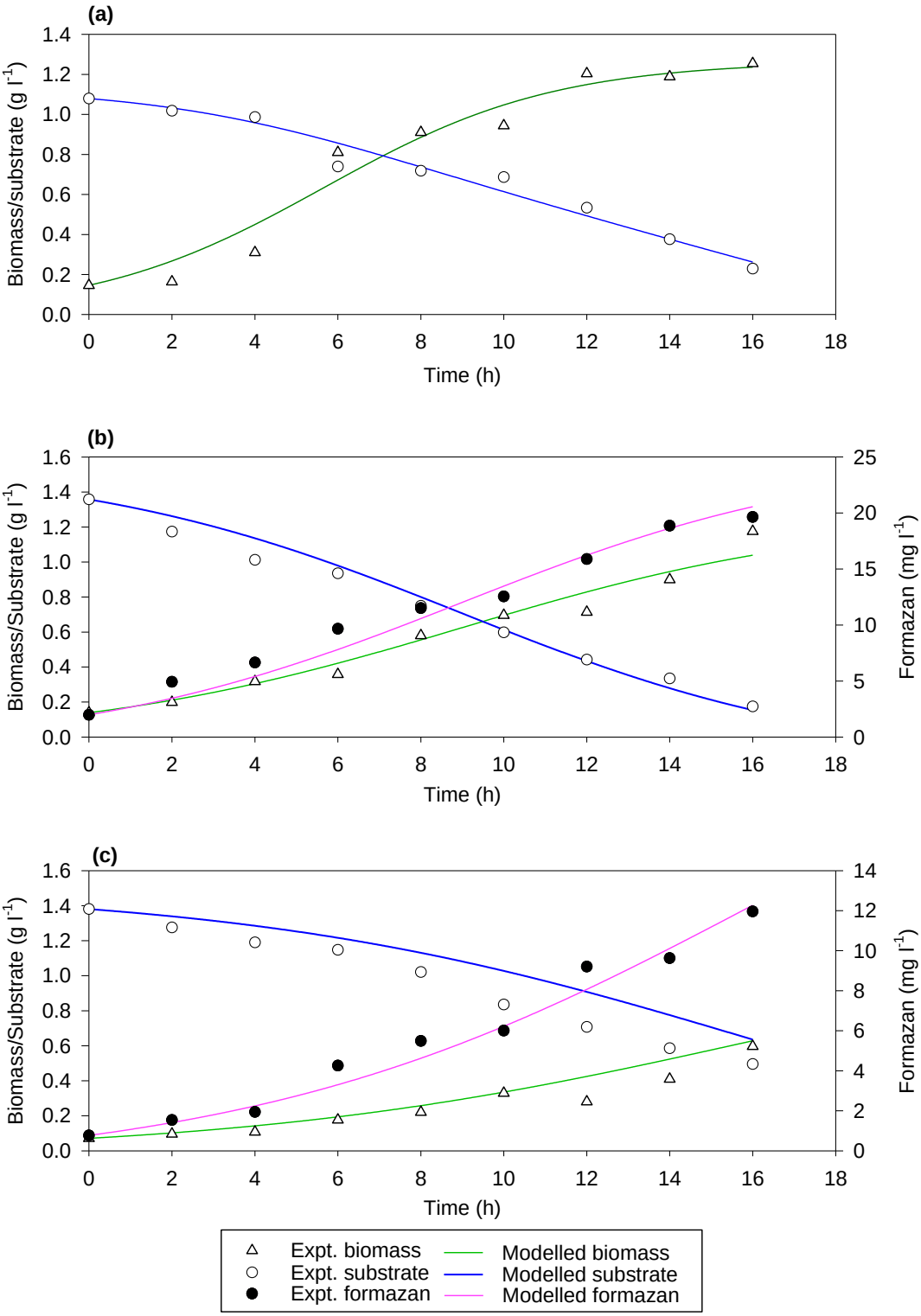

541

542 **Figure 2**. Experimental (symbols) and model-predicted (solid line) profiles for biomass,
543 substrates and formazan concentration (if applicable) in batch studies involving sets with (a)
544 no TTC or toxicant, (b) TTC but no toxicant, and (c) with TTC and toxicant.

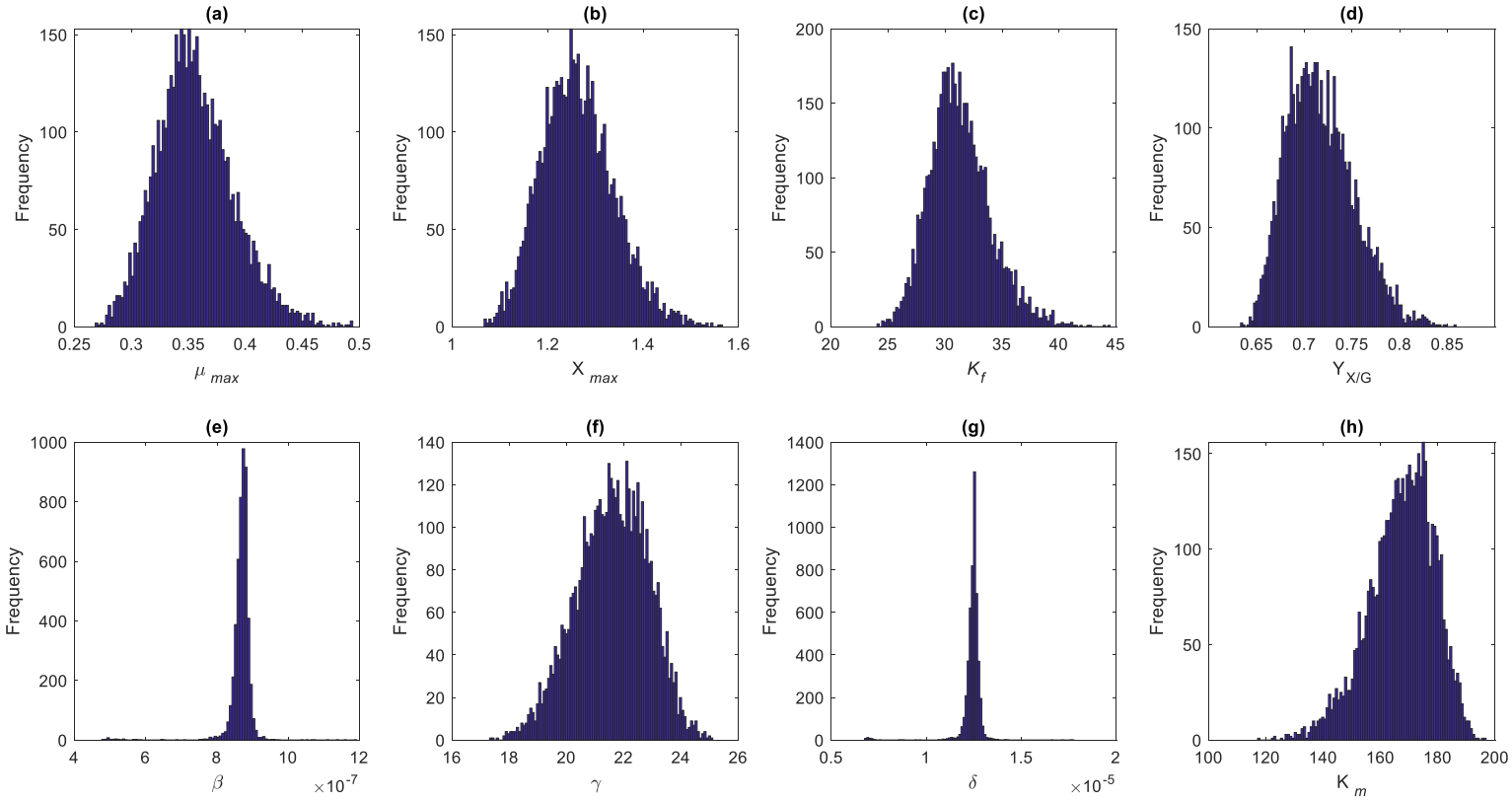

Figure 3. Distribution of bootstrap parameter estimates (N=5000) relevant to microbial growth, substrate consumption, formazan production in the proposed toxicity model.

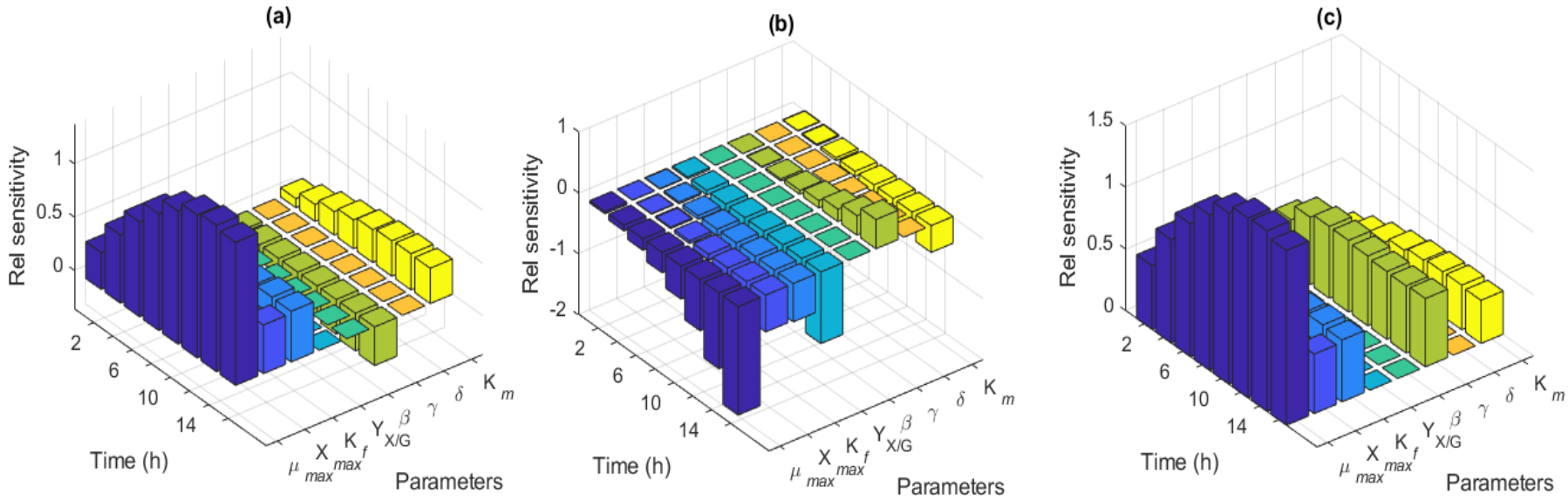

Figure 4. Relative sensitivity of parameters on (a) biomass growth, (b) substrate consumption, and (c) formazan production

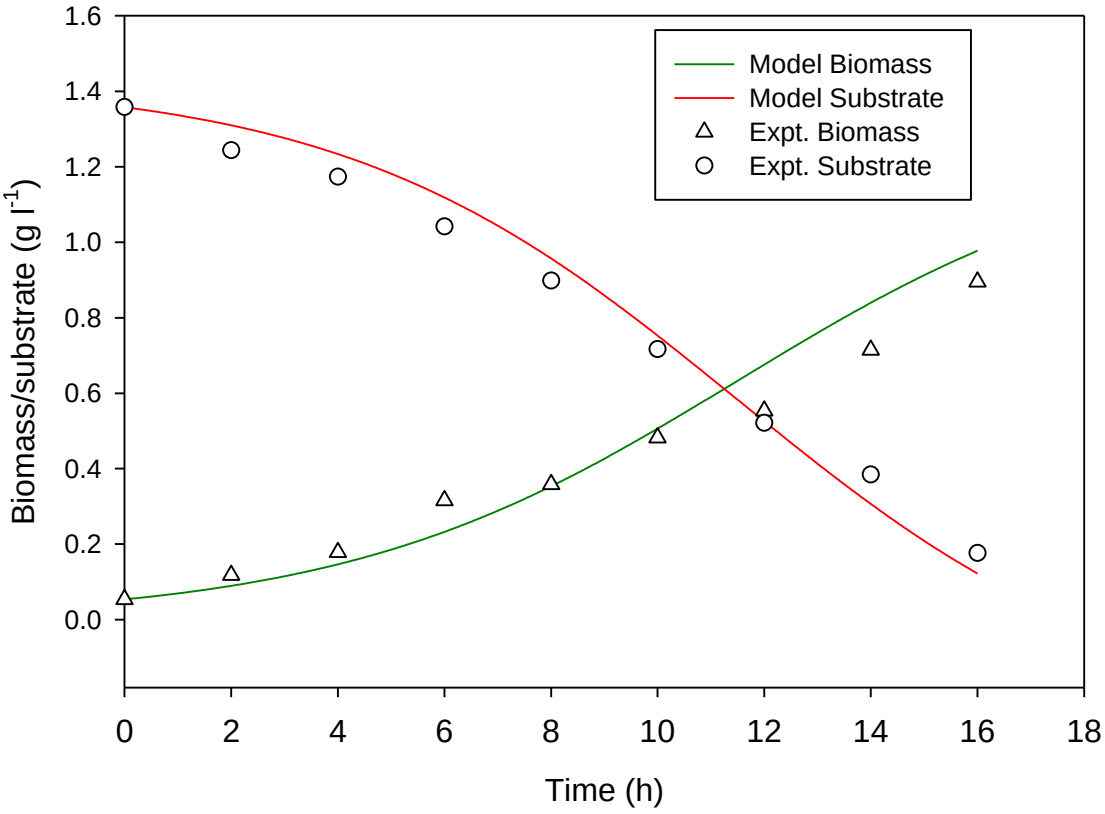

557

558 **Figure 5**. Experimental and modelled biomass and glucose concentration profiles in the

559 validation of toxicity assay model, performed with 50 mg l^{-1} Cu^{2+} in absence of TTC.

560

561

562

563

564